DIGITAL ACCESS TO SCHOLARSHIP AT HARVARD

From Transistor to Trapped-ion Computers for Quantum Chemistry

(Article begins on next page)

From transistor to trapped-ion computers for quantum chemistry

M.-H. Yung[1,2]*, J. Casanova[3]*, A. Mezzacapo[3], J. McClean[2], L. Lamata[3], A. Aspuru-Guzik[2] & E. Solano[3,4]

[1]Center for Quantum Information, Institute for Interdisciplinary Information Sciences, Tsinghua University, Beijing, 100084, P. R. China, [2]Department of Chemistry and Chemical Biology, Harvard University, Cambridge MA, 02138, USA, [3]Department of Physical Chemistry, University of the Basque Country UPV/EHU, Apartado 644, 48080 Bilbao, Spain, [4]IKERBASQUE, Basque Foundation for Science, Alameda Urquijo 36, 48011 Bilbao, Spain.

Correspondence and requests for materials should be addressed to A.A.-G. (aspuru@ chemistry.harvard. edu) or E.S. (enrique. solano@ehu.es)

* These authors contributed equally to this work.

Over the last few decades, quantum chemistry has progressed through the development of computational methods based on modern digital computers. However, these methods can hardly fulfill the exponentially-growing resource requirements when applied to large quantum systems. As pointed out by Feynman, this restriction is intrinsic to all computational models based on classical physics. Recently, the rapid advancement of trapped-ion technologies has opened new possibilities for quantum control and quantum simulations. Here, we present an efficient toolkit that exploits both the internal and motional degrees of freedom of trapped ions for solving problems in quantum chemistry, including molecular electronic structure, molecular dynamics, and vibronic coupling. We focus on applications that go beyond the capacity of classical computers, but may be realizable on state-of-the-art trapped-ion systems. These results allow us to envision a new paradigm of quantum chemistry that shifts from the current transistor to a near-future trapped-ion-based technology.

Quantum chemistry represents one of the most successful applications of quantum mechanics. It provides an excellent platform for understanding matter from atomic to molecular scales, and involves heavy interplay of experimental and theoretical methods. In 1929, shortly after the completion of the basic structure of the quantum theory, Dirac speculated[1] that the fundamental laws for chemistry were completely known, but the application of the fundamental laws led to equations that were too complex to be solved. About ninety years later, with the help of transistor-based digital computers, the development of quantum chemistry continues to flourish, and many powerful methods, such as Hartree-Fock, configuration interaction, density functional theory, coupled-cluster, and quantum Monte Carlo, have been developed to tackle the complex equations of quantum chemistry (see e.g. for a historical review[2]). However, as the system size scales up, all of the methods known so far suffer from limitations that make them fail to maintain accuracy with a finite amount of resources[3]. In other words, quantum chemistry remains a hard problem to be solved by the current computer technology.

As envisioned by Feynman[4], one should be able to efficiently solve problems of quantum systems with a quantum computer. Instead of solving the complex equations, this approach, known as *quantum simulation* (see the recent reviews in Refs. 5–7), aims to solve the problems by simulating target systems with another controllable quantum system, or qubits. Indeed, simulating many-body systems beyond classical resources will be a cornerstone of quantum computers. Quantum simulation is a very active field of study and various methods have been developed. Quantum simulation methods have been proposed for preparing specific states such as ground[8–13] and thermal states[14–20], simulating time evolution[21–27], and the measurement of physical observables[28–31].

Trapped-ion systems (see Fig. 1) are currently one of the most sophisticated technologies developed for quantum information processing[32]. These systems offer an unprecedented level of quantum control, which opens new possibilities for obtaining physico-chemical information about quantum chemical problems. The power of trapped ions for quantum simulation is manifested by the high-precision control over both the internal degrees of freedom of the individual ions and the phonon degrees of freedom of the collective motions of the trapped ions, and the high-fidelity initialization and measurement[32,33]. Up to 100 quantum logic gates have been realized for six qubits with trapped ions[22], and quantum simulators involving 300 ions have been demonstrated[34].

In this work, we present an efficient toolkit for solving quantum chemistry problems based on the state-of-the-art in trapped-ion technologies. The toolkit comprises two components *i*) First, we present a hybrid quantum-classical variational optimization method, called quantum-assisted optimization, for approximating both
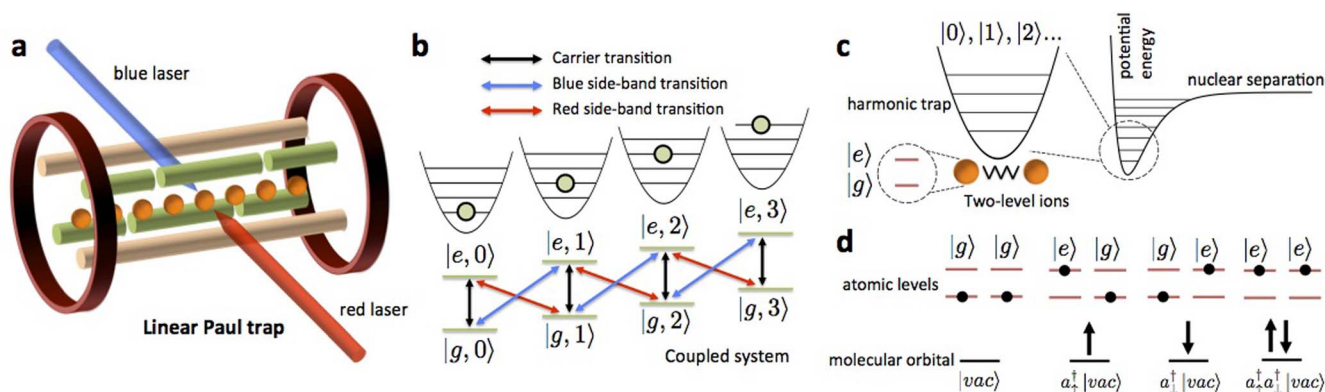
Figure 1 | Simulating quantum chemistry with trapped ions. (a) Scheme of a trapped-ion setup for quantum simulation, which contains a linear chain of trapped ions confined by a harmonic potential, and external lasers that couple the motional and internal degrees of freedom. (b) Transitions between internal and motional degrees of freedom of the ions in the trap. (c) The normal modes of the trapped ions can simulate the vibrational degrees of freedom of molecules. (d) The internal states of two ions can simulate all four possible configurations of a molecular orbital.

ground-state energies and the ground-state eigenvectors for electronic problems. The optimized eigenvector can then be taken as an input for the phase estimation algorithm to project out the exact eigenstates and hence the potential-energy surfaces (see Fig. 2). Furthermore, we extend the application of the unitary coupled-cluster method[35]. This allows for the application of a method developed for classical numerical computations in the quantum domain. *ii*) The second main component of our toolkit is the optimized use of trapped-ion phonon degrees of freedom not only for quantum-gate construction, but also for simulating molecular vibrations, representing a mixed digital-analog quantum simulation. The phonon degrees of freedom in trapped-ion systems provide a natural platform for addressing spin-boson or fermion-boson-type problems through quantum simulation[23,36–40]. It is noteworthy to mention that, contrary to the continuous of modes required for full-fledged quantum field theories, quantum simulations of quantum chemistry problems could reach realistic conditions for finite bosonic and fermionic mode numbers. Consequently, trapped ions can be exploited to solve dynamical problems involving linearly or non-linearly coupled oscillators, e.g., spin-boson models[41,42], that are difficult to solve either analytically or numerically with a classical computer. Furthermore, we have also developed a novel protocol to measure correlation functions of observables in trapped ions that will be crucial for the quantum simulation of quantum chemistry.

Results and Discussion

Trapped ions for quantum chemistry. Quantum chemistry deals with the many-body problem involving electrons and nuclei. Thus, it is very well suited for being simulated with trapped-ion systems, as we will show below. The full quantum chemistry Hamiltonian, $H = T_e + V_e + T_N + V_N + V_{eN}$, is a sum of the kinetic energies of the electrons $T_e \equiv -\frac{\hbar^2}{2m}\sum_i \nabla_{e,i}^2$ and nuclei $T_N \equiv -\sum_i \frac{\hbar^2}{2M_i}\nabla_{N,i}^2$, and the electron-electron $V_e \equiv \sum_{j>i} e^2/|\mathbf{r}_i - \mathbf{r}_j|$, nuclei-nuclei $V_N \equiv \sum_{j>i} Z_i Z_j e^2/|\mathbf{R}_i - \mathbf{R}_j|$, and electron-nuclei $V_{eN} \equiv -\sum_{i,j} Z_j e^2/|\mathbf{r}_i - \mathbf{R}_j|$ potential energies, where $\mathbf{r}$ and $\mathbf{R}$ respectively refer to the electronic and nuclear coordinates.

In many cases, it is more convenient to work on the second-quantization representation for quantum chemistry. The advantage is that one can choose a good fermionic basis set of molecular orbitals, $|p\rangle = c_p^\dagger|vac\rangle$, which can compactly capture the low-energy sector of the chemical system. This kind of second quantized fermionic Hamiltonians are efficiently simulatable in trapped ions[23]. To be more specific, we will choose first $M > N$ orbitals for an N-electron system. Denote $\phi_p(\mathbf{r}) \equiv \langle \mathbf{r}|p\rangle$ as the single-particle wavefunction corresponding to mode p. The electronic part, $H_e(\mathbf{R}) \equiv T_e + V_{eN}(\mathbf{R}) + V_e$, of the Hamiltonian H can be expressed as follows:
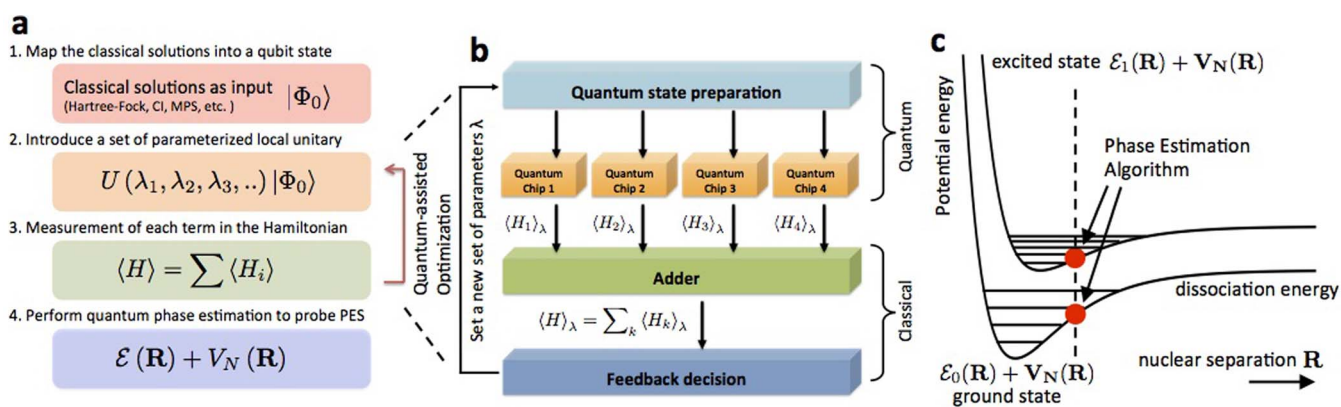
Figure 2 | Outline of the quantum-assisted optimization method. (a) The key steps for quantum assisted optimization, which starts from classical solutions. For each new set of parameters λ's, determined by a classical optimization algorithm, the expectation value $\langle H \rangle$ is calculated. The potential energy surface is then obtained by quantum phase estimation. (b) Quantum measurements are performed for the individual terms in H, and the sum is obtained classically. (c) The same procedure is applied for each nuclear configuration $\mathbf{R}$ to probe the energy surface.

$$H_e(\mathbf{R}) = \sum_{pq} h_{pq} c_p^\dagger c_q + \frac{1}{2} \sum_{pqrs} h_{pqrs} c_p^\dagger c_q^\dagger c_r c_s, \qquad (1)$$

where h_{pq} is obtained from the single-electron integral $h_{pq} \equiv -\int d\mathbf{r} \phi_p^*(\mathbf{r})(T_e + V_{eN})\phi_q(\mathbf{r})$, and h_{pqrs} comes from the electron-electron Coulomb interaction, $h_{pqrs} \equiv \int d\mathbf{r}_1 d\mathbf{r}_2 \phi_p^*(\mathbf{r}_1)\phi_q^*(\mathbf{r}_2)V_e(|\mathbf{r}_1 - \mathbf{r}_2|)\phi_r(\mathbf{r}_2)\phi_s(\mathbf{r}_1)$. We note that the total number of terms in H_e is $O(M^4)$; typically M is of the same order as N. Therefore, the number of terms in H_e scales polynomially in N, and the integrals $\{h_{pq}, h_{pqrs}\}$ can be numerically calculated by a classical computer with polynomial resources[9].

To implement the dynamics associated with the electronic Hamiltonian in Eq. (1) with a trapped-ion quantum simulator, one should take into account the fermionic nature of the operators c_p and $c_q^\dagger$. We invoke the Jordan-Wigner transformation (JWT), which is a method for mapping the occupation representation to the spin (or qubit) representation[43]. Specifically, for each fermionic mode p, an unoccupied state $|0\rangle_p$ is represented by the spin-down state $|\downarrow\rangle_p$, and an occupied state $|1\rangle_p$ is represented by the spin-up state $|\uparrow\rangle_p$. The exchange symmetry is enforced by the Jordan-Wigner transformation: $c_p^\dagger = \left(\prod_{m<p} \sigma_m^z\right)\sigma_p^+$ and $c_p = \left(\prod_{m<p} \sigma_m^z\right)\sigma_p^-$, where $\sigma^\pm \equiv (\sigma^x \pm i\sigma^y)/2$. Consequently, the electronic Hamiltonian in Eq. (1) becomes highly nonlocal in terms of the Pauli operators $\{\sigma^x, \sigma^y, \sigma^z\}$, i.e.,

$$H_e \xrightarrow[\text{JWT}]{} \sum_{i,j,k\ldots \in \{x,y,z\}} g_{ijk\ldots}\left(\sigma_1^i \otimes \sigma_2^j \otimes \sigma_3^k \ldots\right). \qquad (2)$$

Nevertheless, the simulation can still be made efficient with trapped ions, as we shall discuss below.

In trapped-ion physics two metastable internal levels of an ion are typically employed as a qubit. Ions can be confined either in Penning traps or radio frequency Paul traps[33], and cooled down to form crystals. Through sideband cooling the ions motional degrees of freedom can reach the ground state of the quantum Harmonic oscillator, that can be used as a quantum bus to perform gates among the different ions. Using resonance fluorescence with a cycling transition quantum non demolition measurements of the qubit can be performed. The fidelities of state preparation, single- and two-qubit gates, and detection, are all above 99%[32].

The basic interaction of a two-level trapped ion with a single-mode laser is given by[32], $H = \hbar\Omega\sigma_+ e^{-i(\Delta t - \phi)} \exp\left(i\eta\left[ae^{-i\omega_t t} + a^\dagger e^{i\omega_t t}\right]\right) +$ H.c., where $\sigma_\pm$ are the atomic raising and lowering operators, a ($a^\dagger$) is the annihilation (creation) operator of the considered motional mode, and Ω is the Rabi frequency associated to the laser strength. $\eta = kz_0$ is the Lamb-Dicke parameter, with k the wave vector of the laser and $z_0 = \sqrt{\hbar/(2m\omega_t)}$ the ground state width of the motional mode. ϕ is a controllable laser phase and Δ the laser-atom detuning.

In the Lamb-Dicke regime where $\eta\sqrt{\langle(a+a^\dagger)^2\rangle} \ll 1$, the basic interaction of a two-level trapped ion with a laser can be rewritten as $H = \hbar\Omega\left[\sigma_+ e^{-i(\Delta t - \phi)} + i\eta\sigma_+ e^{-i(\Delta t - \phi)}\left(ae^{-i\omega_t t} + a^\dagger e^{i\omega_t t}\right) + \text{H.c.}\right]$

By adjusting the laser detuning Δ, one can generate the three basic ion-phonon interactions, namely: the carrier interaction ($\Delta=0$) $H_c = \hbar\Omega(\sigma_+ e^{i\phi} + \sigma_- e^{-i\phi})$, the red sideband interaction ($\Delta = -\omega_t$) $H_r = i\eta\hbar\Omega(\sigma_+ ae^{i\phi} - \sigma_- a^\dagger e^{-i\phi})$, and the blue sideband interaction ($\Delta = \omega_t$) $H_b = i\eta\hbar\Omega(\sigma_+ a^\dagger e^{i\phi} - \sigma_- ae^{-i\phi})$. By combining detuned red and blue sideband interactions, one obtains the Mølmer-Sørensen gate[44], which is the basic building block for our methods. With combinations of this kind of gates, one can obtain dynamics as

the associated one to H_e in Eq. (2), that will allow one to simulate arbitrary quantum chemistry systems.

Quantum-assisted optimization. Quantum-assisted optimization[45] (see also Fig. 2) for obtaining ground-state energies aims to optimize the use of quantum coherence by breaking down the quantum simulation through the use of both quantum and classical processors; the quantum processor is strategically employed for expensive tasks only.

To be more specific, the first step of quantum-assisted optimization is to prepare a set of quantum states $\{|\psi_\lambda\rangle\}$ that are characterized by a set of parameters $\{\lambda\}$. After the state is prepared, the expectation value $E_\lambda \equiv \langle\psi_\lambda| H |\psi_\lambda\rangle$ of the Hamiltonian H will be measured directly, without any quantum evolution in between. Practically, the quantum resources for the measurements can be significantly reduced when we divide the measurement of the Hamiltonian $H = \sum_i H_i$ into a polynomial number of small pieces $\langle H_i\rangle$ (cf Eq. (2)). These measurements can be performed in a parallel fashion, and no quantum coherence is needed to maintain between the measurements (see Fig. 2a and 2b). Then, once a data point of E_λ is obtained, the whole procedure is repeated for a new state $\{|\psi_\lambda'\rangle\}$ with another set of parameters $\{\lambda'\}$. The choice of the new parameters is determined by a classical optimization algorithm that aims to minimize E_λ (see Methods). The optimization procedure is terminated after the value of E_λ converges to some fixed value.

Finally, for electronic Hamiltonians $H_e(\mathbf{R})$, the optimized state can then be sent to a quantum circuit of phase estimation algorithm to produce a set of data point for some $\mathbf{R}$ on the potential energy surfaces (Fig. 2c shows the 1D case). After locating the local minima of the ground and excited states, vibronic coupling for the electronic structure can be further studied (see Supplementary Material).

The performance of quantum-assisted optimization depends crucially on (a) the choice of the variational states, and (b) efficient measurement methods. We found that the unitary coupled-cluster (UCC) states[35] are particularly suitable for being the input state for quantum-assisted optimization, where each quantum state $|\psi_\lambda\rangle$ can be prepared efficiently with standard techniques in trapped ions. Furthermore, efficient measurement methods for H_e are also available for trapped ion systems. We shall discuss these results in detail in the following sections.

Unitary coupled-cluster (UCC) ansatz. The unitary coupled-cluster (UCC) ansatz[35] assumes electronic states $|\psi\rangle$ have the following form, $|\psi\rangle = e^{T - T^\dagger}|\Phi\rangle$, where $|\Phi\rangle$ is a reference state, which can be, e.g., a Slater determinant constructed from Hartree-Fock molecular orbitals. The particle-hole excitation operator, or cluster operator T, creates a linear combination of excited Slater determinants from $|\Phi\rangle$. Usually, T is divided into subgroups based on the particle-hole rank. More precisely, $T = T_1 + T_2 + T_3 + \ldots + T_N$ for an N-electron system, where $T_1 = \sum_{i,a} t_i^a c_a^\dagger c_i$, $T_2 = \sum_{i,j,a,b} t_{ij}^{ab} c_a^\dagger c_b^\dagger c_j c_i$, and so on.

Here $c_a^\dagger$ creates an electron in the orbital a. The indices a, b label unoccupied orbitals in the reference state $|\Phi\rangle$, and i, j label occupied orbitals. The energy obtained from UCC, namely $E = \langle\Phi|e^{T^\dagger - T} H e^{T - T^\dagger}|\Phi\rangle$ is a variational upper bound of the exact ground-state energy.

The key challenge for implementing UCC on a classical computer is that the computational resource grows exponentially. It is because, in principle, one has to expand the expression $\tilde{H} \equiv e^{T^\dagger - T} H e^{T - T^\dagger}$ into an infinity series, using the Baker-Campbell-Hausdorff expansion. Naturally, one has to rely on approximate methods[35,46] to truncate the series and keep track of finite numbers of terms. Therefore, in order to make good approximations by perturbative methods, i.e., assuming T is small, one implicitly assumes that the reference state $|\Phi\rangle$ is a good solution to the problem. However, in many cases, such an assumption is not valid and the use of approximate UCC breaks

down. We explain below how implementing UCC on a trapped-ion quantum computer can overcome this problem.

Implementation of UCC through time evolution. We can generate the UCC state by simulating a pseudo time evolution through Suzuki-Trotter expansion on the evolution operator $e^{T-T^\dagger}$[21]. To proceed, we consider an N-electron system with M, where $M > N$, molecular orbitals (including spins). We need totally M qubits; the reference state is the Hartree-Fock state where N orbitals are filled, and $M - N$ orbitals are empty, i.e, $|\Phi\rangle = |000...0111...1\rangle$. We also define an effective Hamiltonian $K \equiv i(T - T^\dagger)$, which means that we should prepare the state $e^{-iK}|\Phi\rangle$.

We decompose K into subgroups $K = K_1 + K_2 + K_3 + ... + K_P$, where $P \leq N$, and $K_i \equiv i\left(T_i - T_i^\dagger\right)$. We now write $e^{-iK} = (e^{-iK\delta})^{1/\delta}$ for some dimensionless constant δ. For small δ, we have $e^{-iK} \approx e^{-iK_P\delta} \cdots e^{-iK_2\delta} e^{-iK_1\delta}$. Since each K_j contains $N^j(M-N)^j$ terms of the creation $c^\dagger$ and annihilation c operators, we will need to individually simulate each term separately, e.g., $e^{-i\left(tc_a^\dagger c_i - t^* c_i^\dagger c_a\right)}$ and $e^{-i\left(tc_a^\dagger c_b^\dagger c_j c_i - t^* c_i^\dagger c_j^\dagger c_b c_a\right)}$, which can be implemented by transforming into spin operators through Jordan-Wigner transformation. The time evolution for each term can be simulated with a quantum circuit involving many nonlocal controlled gates, which can be efficiently implemented with trapped ions as we shall see below.

Implementation of UCC and simulation of time evolution with trapped-ions. Our protocol for implementing the UCC ansatz requires the simulation of the small-time t/n evolution of non-local product of Pauli matrices of the form: $e^{-iH_l t/n}$, where $H_l = g_l \sigma_1^i \sigma_2^j \sigma_3^k \cdots$ for $i, j, k \in \{x, y, z\}$. Note that for any N-spin interaction, the $e^{-iH_l t/n}$ terms are equivalent to $e^{i\phi \sigma_1^x \sigma_2^x \sigma_3^x \cdots \sigma_N^x}$ through local spin rotations, which are simple to implement on trapped ions. Such a non-local operator can be implemented using the multi-particle Mølmer-Sørensen gate[23,39]: $U_{MS}(\theta, \varphi) \equiv \exp\left[-i\theta(\cos\varphi S_x + \sin\varphi S_y)^2/4\right]$, where $S_{x,y} \equiv \sum_i \sigma_i^{x,y}$ is a collective spin operator. Explicitly,

$$e^{i\phi \sigma_1^z \sigma_2^x \sigma_3^x \cdots \sigma_N^x} = U_{MS}\left(\frac{-\pi}{2}, 0\right) R_N(\phi) U_{MS}\left(\frac{\pi}{2}, 0\right). \quad (3)$$

Here $R_N(\phi)$ is defined as follows: for any $m \in \mathbb{N}$, $R_N(\phi) = e^{\pm i\phi \sigma_1^z}$ for $N = 4m \pm 1$, and (ii) $R_N(\phi) = e^{i\phi \sigma_1^y}$ for $N = 4m$, and (iii) $R_N(\phi) = e^{-i\phi \sigma_1^y}$ for $N = 4m - 2$.

It is remarkable that the standard quantum-circuit treatment (e.g. see Ref.[47]) for implementing each $e^{-iH_l t/n}$ involves as many as $2N$ two-qubit gates for simulating N fermionic modes; in our protocol one needs only two Mølmer-Sørensen gates, which are straightforwardly implementable with current trapped-ion technology. Furthermore, the local rotation $R_N(\phi)$ can also include motional degrees of freedom of the ions for simulating arbitrary fermionic Hamiltonians coupled linearly to bosonic operators a_k and $a_k^\dagger$.

Measurement of arbitrarily-nonlocal spin operators. For any given state $|\psi\rangle$, we show how to encode expectation value of products of Pauli matrices $\left\langle \sigma_1^i \otimes \sigma_2^j \otimes \sigma_3^k \otimes \cdots \right\rangle \equiv \langle\psi|\sigma_1^i \otimes \sigma_2^j \otimes \sigma_3^k \otimes \cdots|\psi\rangle$, where $i, j, k \in \{x, y, z\}$, onto an expectation value of a single qubit. The idea is to first apply the unitary evolution of the form: $e^{-i\theta\left(\sigma_1^i \otimes \sigma_2^j \otimes \cdots\right)}$, which as we have seen (cf Eq. 3) can be generated by trapped ions efficiently, to the state $|\psi\rangle$ before the measurement. For example, defining $|\psi_\theta\rangle \equiv e^{-i\theta\left(\sigma_1^x \otimes \sigma_2^x \otimes \cdots\right)}|\psi\rangle$, we have the relation

$$\langle\psi_\theta|\sigma_1^z|\psi_\theta\rangle = \cos(2\theta)\langle\sigma_1^z\rangle + \sin(2\theta)\langle\sigma_1^y \otimes \sigma_2^x \otimes \cdots\rangle, \quad (4)$$

which equals $\langle\psi|\left(\sigma_1^y \otimes \sigma_2^x \otimes \ldots\right)|\psi\rangle$ for $\theta = \pi/4$. Note that the application of this method requires the measurement of one qubit

only, making this technique especially suited for trapped ion systems where the fidelity of the measurement of one qubit is 99.99%[48].

This method can be further extended to include bosonic operators in the resulting expectation values. For example, re-define $|\psi_\theta\rangle = e^{-i\theta\left(\sigma_1^i \otimes \sigma_2^j \otimes \cdots\right) \otimes \left(a + a^\dagger\right)}|\psi\rangle$ and consider $\theta \to \theta(a + a^\dagger)$ in Eq. (4). We can obtain the desired correlation through the derivative of the single-qubit measurement: $\partial_\theta\langle\psi_\theta|\sigma_1^z|\psi_\theta\rangle|_{\theta=0} = -2\left\langle\left(\sigma_1^y \otimes \sigma_2^x \otimes \cdots\right)\left(a + a^\dagger\right)\right\rangle$. Note that the evolution operator of the form $e^{-i\theta\left(\sigma_1^i \otimes \sigma_2^j \otimes \cdots\right) \otimes \left(a + a^\dagger\right)}$ can be generated by replacing the local operation $R_N(\phi)$ in Eq. 3 with $e^{\pm i\phi \sigma_1^i \left(a + a^\dagger\right)}$. This technique allows us to obtain a diverse range of correlations between bosonic and internal degrees of freedom.

Probing potential energy surfaces. In the Born-Oppenheimer (BO) picture, the potential energy surface $\mathcal{E}_k(\mathbf{R}) + V_N(\mathbf{R})$ associated with each electronic eigenstate $|\phi_k\rangle$ is obtained by scanning the eigenvalues $\mathcal{E}_k(\mathbf{R})$ for each configurations of the nuclear coordinates $\{\mathbf{R}\}$. Of course, we can apply the standard quantum phase estimation algorithm[49] that allows us to extract the eigenvalues. However, this can require many ancilla qubits. In fact, locating these eigenvalues can be achieved by the phase estimation method utilizing one extra ancilla qubit[12] corresponding, in our case, to one additional ion.

This method works as follows: suppose we are given a certain quantum state $|\psi\rangle$ (which may be obtained from classical solutions with quantum-assisted optimization) and an electronic Hamiltonian $H_e(\mathbf{R})$ (cf. Eq. (1)). Expanding the input state, $|\psi\rangle = \sum_k \alpha_k |\phi_k\rangle$, by the eigenstate vectors $|\phi_k\rangle$ of $H_e(\mathbf{R})$, where $H_e(\mathbf{R})|\phi_k\rangle = \mathcal{E}_k(\mathbf{R})|\phi_k\rangle$, then for the input state $|0\rangle|\psi\rangle$, the quantum circuit of the quantum phase estimation produces the following output state, $\left(1/\sqrt{2}\right)\sum_k \alpha_k\left(|0\rangle + e^{-i\omega_k t}|1\rangle\right)|\phi_k\rangle$, where $\omega_k = \mathcal{E}_k/\hbar$. The corresponding reduced density matrix,

$$\frac{1}{2}\begin{pmatrix} 1 & \sum_k |\alpha_k|^2 e^{i\omega_k t} \\ \sum_k |\alpha_k|^2 e^{-i\omega_k t} & 1 \end{pmatrix}, \quad (5)$$

of the ancilla qubit contains the information about the weight (amplitude-square) $|\alpha_k|^2$ of the eigenvectors $|\phi_k\rangle$ in $|\psi\rangle$ and the associated eigenvalues ω_k in the off-diagonal matrix elements. All $|\alpha_k|^2$'s and ω_k's can be extracted by repeating the quantum circuit for a range of values of t and performing a (classical) Fourier transform to the measurement results. The potential energy surface is obtained by repeating the procedure for different values of the nuclear coordinates $\{\mathbf{R}\}$.

Numerical investigation. In order to show the feasibility of our protocol, we can estimate the trapped-ion resources needed to simulate, e.g., the prototypical electronic Hamiltonian $H_e = \sum h_{pq} a_p^\dagger a_q + (1/2)\sum h_{pqrs} a_p^\dagger a_q^\dagger a_r a_s$ as described in Eq. (1), for the specific case of the H_2 molecule in a minimal STO-3G basis. This is a two-electron system represented in a basis of four spin-orbitals. The hydrogen atoms were separated by 0.75 Å, near the equilibrium bond distance of the molecule. The Hamiltonian is made up of 12 terms, that include 4 local ion operations and 8 non-local interactions. Each of the non-local terms can be done as a combination of two Mølmer-Sørensen (MS) gates and local rotations, as described in Table 1. Therefore, to implement the dynamics, one needs 16 MS gates per Trotter step and a certain number of local rotations upon the ions. Since $\pi/2$ MS gates can be done in ~ 50 μs, and local rotations can be performed in negligible times (~ 1 μs)[22,32], the total simulation time can be assumed of about 800 μs for the $n=1$ protocol, 1.6 ms and 2.4 ms for the $n=2$ and $n=3$ protocols. Thus total simulation times are within the decoherence times for trapped-ion setups, of about 30 ms[32]. In a digital protocol performed on real

Table 1 | Using trapped ions to simulate quantum chemistry

	Simulating Quantum Chemistry	Implementation with Trapped Ions
Hamiltonian transformation:	The fermionic (electronic) Hamiltonian H_e is transformed into a spin Hamiltonian through the Jordan-Wigner transformation. $$H_e \rightarrow \sum_{i,j,k,\dots \in (x,y,z)} g_{ijk\dots} \left(\sigma_1^i \otimes \sigma_2^j \otimes \sigma_3^k \cdots \right) \equiv \sum_{l=1}^m H_l$$	The spin degrees of freedom in H_e are represented by the internal degrees of freedom of the trapped ions.
Simulation of time evolution:	The time evolution operator $e^{-iH_t t}$ is split into n small-time (t/n) pieces $e^{-iH_t t/n}$ through the Suzuki-Trotter expansion. $$e^{-i\sum_{l=1}^m H_l t} = \left(e^{-iH_1 t/n} e^{-iH_2 t/n} \cdots e^{-iH_m t/n} \right)^n$$	Each individual term $e^{-iH_l t/n}$ can be simulated with trapped ions through the use of Mølmer-Sørensen gates U_{MS}. Explicitly, $$e^{-iH_l t/n} = U_{MS}\left(\frac{-\pi}{2}, 0 \right) U_{\sigma_z}(\phi) U_{MS}\left(\frac{\pi}{2}, 0 \right).$$
Obtaining average energy:	The average energy $\langle H_e \rangle$ of the Hamiltonian can be obtained through the sum of the individual terms $\langle H_l \rangle$, which reduces to the measurement of products of Pauli matrices.	For any prepared state $|\psi\rangle$, average values of the products of Pauli matrices $J_{ijk\dots} \equiv \sigma_1^i \otimes \sigma_2^j \otimes \sigma_3^k \cdots$ can be measured by first applying the pseudo time evolution operator $e^{-i(\pi/4)J_{ijk\dots}}$ to $|\psi\rangle$ and then measuring $\langle \sigma_1^z \rangle$.
Measuring eigenvalues:	The eigenvalues of the Hamiltonian can be obtained through the phase estimation algorithm. Good trial states can be obtained through classical computing, or the unitary coupled-cluster method.	The phase estimation algorithm can be implemented through the simulation of controlled time evolutions.
Molecular vibrations:	The inclusion of vibrational degrees of freedom is necessary for corrections on the Born-Oppenheimer picture in the electronic structure of molecules.	The vibrational degrees of freedom are represented by the quantized vibrational motion of the trapped ions.

quantum systems, each gate is affected by an error. Thus, increasing the number of Trotter steps leads to an accumulation of the single gate error. To implement an effective quantum simulation, on one hand one has to increase the number of steps to reduce the error due to the digital approximation, on the other hand one is limited by the accumulation of the single gate error. We plot in Fig. 3a, 3b, 3c, the fidelity loss $1 - |\langle \Psi_S | \Psi_E \rangle|^2$ of the simulated state $|\Psi_S\rangle$ versus the exact one $|\Psi_E\rangle$, for the hydrogen Hamiltonian, starting from the initial state with two electrons in the first two orbitals. We plot, along with the digital error, three horizontal lines representing the accumulated gate error, for $n = 1, 2, 3$ in each plot, considering a protocol with an error per Trotter step of $\epsilon = 10^{-3}$ (a), $\epsilon = 10^{-4}$ (b) and $\epsilon = 10^{-5}$ (c). To achieve a reasonable fidelity, one has to find a number of steps that fits the simulation at a specific time. The vertical lines and arrows in the figure mark the time regions in which the error starts to be dominated by the digital error. Trapped-ion two-qubit gates are predicted to achieve in the near future infidelities of 10^{-4}, thus making the use of these protocols feasible[50]. In Fig. 3d we plot the behavior of the energy of the system for the initial state $|\uparrow\uparrow\downarrow\downarrow\rangle$ for the exact dynamics, versus the digitized one. Again, one can observe how the energy can be retrieved with a small error within a reduced number of digital steps.

Conclusions

Summarizing, we have proposed a quantum simulation toolkit for quantum chemistry with trapped ions. This paradigm in quantum simulations has several advantages: an efficient electronic simulation, the possibility of interacting electronic and vibrational degrees of freedom, and the increasing scalability provided by trapped-ion systems. This approach for solving quantum chemistry problems aims to combine the best of classical and quantum computation.

Methods

To implement the optimization with the UCC wavefunction ansatz on a trapped-ion quantum simulator, our proposal is to first employ classical algorithms to obtain approximate solutions[35,46]. Then, we can further improve the quality of the solution by searching for the true minima with an ion trap. The idea is as follows: first we create a UCC ansatz by the Suzuki-Trotter method described in the previous section. Denote this choice of the cluster operator as $T^{(0)}$, and other choices as $T^{(k)}$ with $k = 1, 2, 3, \dots$. The corresponding energy $E_0 = \langle \Phi | e^{T^{(0)\dagger} - T^{(0)}} H e^{T^{(0)} - T^{(0)\dagger}} | \Phi \rangle$ of the initial state is obtained by a classical computer.

Next, we choose another set of cluster operator $T^{(1)}$ which is a perturbation around $T^{(0)}$. Define the new probe state $|\phi_k\rangle \equiv e^{T^{(k)} - T^{(k)\dagger}} |\Phi\rangle$. Then, the expectation value of the energy $E_1 = \langle \Phi | e^{T^{(1)\dagger} - T^{(1)}} H e^{T^{(1)} - T^{(1)\dagger}} | \Phi \rangle = \langle \phi_1 | H | \phi_1 \rangle$ can be obtained by measuring components of the second quantized Hamiltonian, $\langle \phi_1 | H | \phi_1 \rangle = \sum_{pqrs} \tilde{h}_{pqrs} \langle \phi_1 | c_p^\dagger c_q^\dagger c_r c_s | \phi_1 \rangle$. Recall that the coefficients $\tilde{h}_{pqrs}$ are all precomputed and known.

In order to obtain measurement results for the operators $\langle \phi_1 | c_p^\dagger c_q^\dagger c_r c_s | \phi_1 \rangle$, we will first convert the fermion operators into spin operators via Jordan-Wigner transformation; the same procedure is applied for creating the state $|\phi_1\rangle$. The quantum measurement for the resulting products of Pauli matrices can be achieved efficiently with trapped ions, using the method we described.

The following steps are determined through a classical optimization algorithm. There can be many choices for such an algorithm, for example gradient descent method, Nelder-Mead method, or quasi-Newton methods. For completeness, we summarize below the application of gradient descent method to our optimization problem.

First we define the vector $\mathbf{T}^{(k)} = \left(t_i^{a(k)}, t_{ij}^{ab(k)}, \dots \right)^T$ to contain all coefficients in the cluster operator $T^{(k)}$ at the k-th step. We can also write the expectation value $E(\mathbf{T}^{(k)}) \equiv \langle \phi_k | H | \phi_k \rangle$ for each step as a function of $\mathbf{T}^{(k)}$. The main idea of the gradient descent method is that $E(\mathbf{T}^{(k)})$ decreases fastest along the direction of the negative gradient of $E(\mathbf{T}^{(k)})$, $-\nabla E(\mathbf{T}^{(k)})$. Therefore, the $(k + 1)$-th step is determined by the following relation:

$$\mathbf{T}^{(k+1)} = \mathbf{T}^{(k)} - a_k \nabla E\left(\mathbf{T}^{(k)} \right), \qquad (6)$$

where a_k is an adjustable parameter; it can be different for each step. To obtain values of the gradient $\nabla E(\mathbf{T}^{(k)})$, one may use the finite-difference method to approximate the gradient. However, numerical gradient techniques are often susceptible to numerical instability. Alternatively, we can invoke the Hellman-Feynman theorem and get, e.g.,
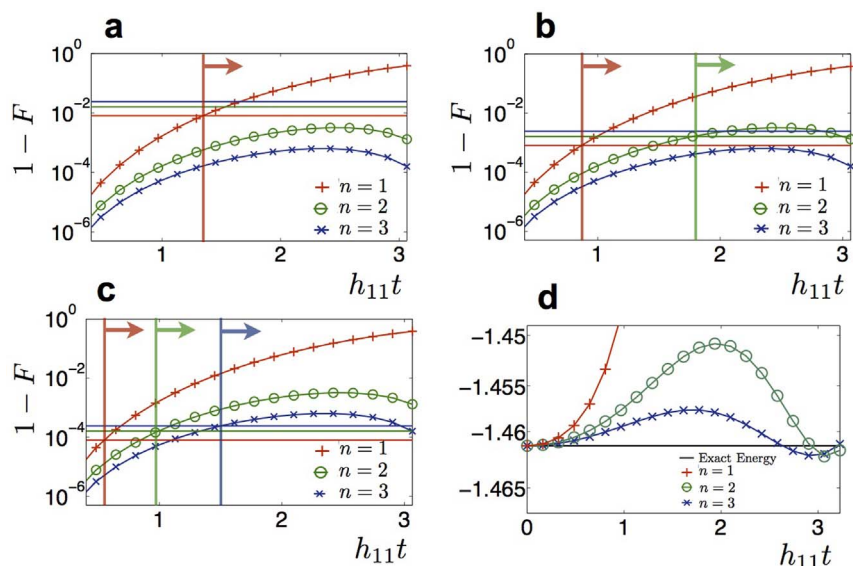
Figure 3 | Digital error $1 - F$ (curves) along with the accumulated gate error (horizontal lines) versus time in h_{11} energy units, for $n = 1, 2, 3$ Trotter steps in each plot, considering a protocol with an error per Trotter step of $\epsilon = 10^{-3}$ (a), $\epsilon = 10^{-4}$ (b) and $\epsilon = 10^{-5}$ (c). The initial state considered is $|\uparrow\uparrow\downarrow\downarrow\rangle$, in the qubit representation of the Hartree-Fock state in a molecular orbital basis with one electron on the first and second orbital. Vertical lines and arrows define the time domain in which the dominant part of the error is due to the digital approximation. d) Energy of the system, in h_{11} units, for the initial state $|\uparrow\uparrow\downarrow\downarrow\rangle$ for the exact dynamics, versus the digitized one. For a protocol with three Trotter steps the energy is recovered up to a negligible error.

$\left(\partial/\partial t_i^a\right) E\left(\mathbf{T}^{(k)}\right) = \langle \phi_k | \left[H, c_a^\dagger c_i\right] | \phi_k \rangle$, which can be obtained with a method similar to that for obtaining $E(\mathbf{T}^{(k)})$.

Finally, as a valid assumption for general cases, we assume our parametrization of UCC gives a smooth function for $E(\mathbf{T}^{(k)})$. Thus, it follows that $E\left(\mathbf{T}^{(0)}\right) \geq E\left(\mathbf{T}^{(1)}\right) \geq E\left(\mathbf{T}^{(2)}\right) \geq \cdots$, and eventually $E\left(\mathbf{T}^{(k)}\right)$ converges to a minimum value for large k. Finally, we can also obtain the optimized UCC quantum state.

1. Dirac, P. A. M. Quantum Mechanics of Many-Electron Systems. *Proc. R. Soc. A* **123**, 714–733 (1929).
2. Love, P. J. Back to the Future: A roadmap for quantum simulation from vintage quantum chemistry. eprint arXiv:1208.5524 (2012). (To Appear in Advances in Chemical Physics).
3. Head-Gordon, M. & Artacho, E. Chemistry on the computer. *Phys. Today,* **61**, 58 (2008).
4. Feynman, R. P. Simulating physics with computers. *Int. J. Theor. Phys.* **21**, 467–488 (1982).
5. Kassal, I., Whitfield, J. D., Perdomo-Ortiz, A., Yung, M.-H. & Aspuru-Guzik, A. Simulating chemistry using quantum computers. *Annu. Rev. Phys. Chem.* **62**, 185207 (2011).
6. Yung, M.-H., Whitfield, J. D., Boixo, S., Tempel, D. G. & Aspuru-Guzik, A. Introduction to Quantum Algorithms for Physics and Chemistry. eprint arXiv:1203.1331 (2012).
7. Aspuru-Guzik, A. & Walther, P. Photonic quantum simulators. *Nat. Phys.* **8**, 285291 (2012).
8. Abrams, D. & Lloyd, S. Quantum Algorithm Providing Exponential Speed Increase for Finding Eigenvalues and Eigenvectors. *Phys. Rev. Lett.* **83**, 5162–5165 (1999).
9. Aspuru-Guzik, A., Dutoi, A. D., Love, P. J. & Head-Gordon, M. Simulated quantum computation of molecular energies. *Science* **309**, 1704–7 (2005).
10. Lanyon, B. P. *et al.* Towards quantum chemistry on a quantum computer. *Nat. Chem.* **2**, 106–11 (2010).
11. Poulin, D. & Wocjan, P. Preparing Ground States of Quantum Many-Body Systems on a Quantum Computer. *Phys. Rev. Lett.* **102**, 130503 (2009).
12. Li, Z. *et al.* Solving quantum ground-state problems with nuclear magnetic resonance. *Sci. Rep.* **1**, 88 (2011).
13. Xu, J.-S. *et al.* Demon-like Algorithmic Quantum Cooling and its Realization with Quantum Optics.eprint arXiv:1208.2256 (2012).
14. Lidar, D. & Biham, O. Simulating Ising spin glasses on a quantum computer. *Phys. Rev. E* **56**, 3661–3681 (1997).
15. Poulin, D. & Wocjan, P. Sampling from the Thermal Quantum Gibbs State and Evaluating Partition Functions with a Quantum Computer. *Phys. Rev. Lett.* **103**, 220502 (2009).
16. Yung, M.-H., Nagaj, D., Whitfield, J. & Aspuru-Guzik, A. Simulation of classical thermal states on a quantum computer: A transfer-matrix approach. *Phys. Rev. A* **82**, 060302 (2010).
17. Bilgin, E. & Boixo, S. Preparing Thermal States of Quantum Systems by Dimension Reduction. *Phys. Rev. Lett.* **105**, 170405 (2010).
18. Temme, K., Osborne, T. J., Vollbrecht, K. G., Poulin, D. & Verstraete, F. Quantum Metropolis sampling. *Nature* **471**, 87–90 (2011).
19. Yung, M.-H. & Aspuru-Guzik, A. A quantum-quantum Metropolis algorithm. *PNAS* **109**, 754–9 (2012).
20. Zhang, J., Yung, M.-H., Laflamme, R., Aspuru-Guzik, A. & Baugh, J. Digital quantum simulation of the statistical mechanics of a frustrated magnet. *Nat. Comm.* **3**, 880 (2012).
21. Lloyd, S. Universal Quantum Simulators. *Science* **273**, 1073–1078 (1996).
22. Lanyon, B. P. *et al.* Universal digital quantum simulation with trapped ions. *Science* **334**, 57–61 (2011).
23. Casanova, J., Mezzacapo, A., Lamata, L. & Solano, E. Quantum Simulation of Interacting Fermion Lattice Models in Trapped Ions. *Phys. Rev. Lett.* **108**, 190502 (2012).
24. Zalka, C. Simulating quantum systems on a quantum computer. *Proc R. Soc. A* **454**, 313–322 (1998).
25. Wu, L.-A., Byrd, M. & Lidar, D. Polynomial-Time Simulation of Pairing Models on a Quantum Computer. *Phys. Rev. Lett.* **89**, 057904 (2002).
26. Kassal, I., Jordan, S. P., Love, P. J., Mohseni, M. & Aspuru-Guzik, A. Polynomial-time quantum algorithm for the simulation of chemical dynamics. *PNAS* **105**, 18681–6 (2008).
27. Childs, A. M. & Kothari, R. Simulating sparse Hamiltonians with star decompositions. *Theory of Quantum Computation Communication and Cryptography TQC 2010* **6519**:94–103, 2011.
28. Lidar, D. & Wang, H. Calculating the thermal rate constant with exponential speedup on a quantum computer. *Phys. Rev. E* **59**, 2429–2438 (1999).
29. Master, C., Yamaguchi, F. & Yamamoto, Y. Efficiency of free-energy calculations of spin lattices by spectral quantum algorithms. *Phys. Rev. A* **67**, 032311 (2003).
30. Kassal, I. & Aspuru-Guzik, A. Quantum algorithm for molecular properties and geometry optimization. *J. Chem. Phys.* **131**, 224102 (2009).
31. Wocjan, P., Chiang, C.-F., Nagaj, D. & Abeyesinghe, A. Quantum algorithm for approximating partition functions. *Phys. Rev. A* **80**, 022340 (2009).
32. Häffner, H., Roos, C. F. & Blatt, R. Quantum computing with trapped ions. *Phys. Rep.* **469**, 155–203 (2008).
33. Leibfried, D., Blatt, R., Monroe, C. & Wineland, D. Quantum dynamics of single trapped ions. *Rev. Mod. Phys.* **75**, 281–324 (2003).
34. Britton, J. W. *et al.* Engineered two-dimensional Ising interactions in a trapped-ion quantum simulator with hundreds of spins. *Nature* **484**, 489–492 (2012).
35. Taube, A. G. & Bartlett, R. J. New perspectives on unitary coupled-cluster theory. *Int. J. Quant. Chem.* **106**, 3393–3401 (2006).
36. Lamata, L., León, J., Schätz, T. & Solano, E. Dirac Equation and Quantum Relativistic Effects in a Single Trapped Ion. *Phys. Rev. Lett.* **98**, 253005 (2007).
37. Gerritsma, R. *et al.* Quantum simulation of the Dirac equation. *Nature* **463**, 68–71 (2010).
38. Casanova, J. *et al.* Quantum Simulation of Quantum Field Theories in Trapped Ions. *Phys. Rev. Lett.* **107**, 260501 (2011).

39. Müller, M., Hammerer, K., Zhou, Y. L., Roos, C. F. & Zoller, P. Simulating open quantum systems: from many-body interactions to stabilizer pumping. *New J. Phys.* **13**, 085007 (2011).

40. Mezzacapo, A., Casanova, J., Lamata, L. & Solano, E. Digital Quantum Simulation of the Holstein Model in Trapped Ions. *Phys. Rev. Lett.* **109**, 200501 (2012).

41. Leggett, A. *et al.* Dynamics of the dissipative two-state system. *Rev. Mod. Phys.* **59**, 185 (1987).

42. Mostame, S. *et al.* Quantum simulator of an open quantum system using superconducting qubits: exciton transport in photosynthetic complexes. *New J. Phys.* **14**, 105013 (2012).

43. Ortiz, G., Gubernatis, J., Knill, E. & Laflamme, R. Quantum algorithms for fermionic simulations. *Phys. Rev. A* **64**, 022319 (2001).

44. Mølmer, K. & Sørensen, A. Multiparticle Entanglement of Hot Trapped Ions. *Phys. Rev. Lett.* **82**, 1835 (1999).

45. Peruzzo, A. *et al.* A variational eigenvalue solver on a quantum processor. eprint arXiv,1304.3061 (2013).

46. Kutzelnigg, W. Error analysis and improvements of coupled-cluster theory. *Theor. Chim. Acta* **80**, 349–386 (1991).

47. Whitfield, J. D., Biamonte, J. & Aspuru-Guzik, A. Simulation of electronic structure Hamiltonians using quantum computers. *Mol. Phys.* **109**, 735750 (2011).

48. Myerson, A. H. *et al.* High-Fidelity Readout of Trapped-Ion Qubits. *Phys. Rev. Lett.* **100**, 200502 (2008).

49. Kaye, P., Laflamme, R. & Mosca, M. *An introduction to quantum computing.* (Oxford University Press, USA, 2007).

50. Kirchmair, G. *et al.* Deterministic entanglement of ions in thermal states of motion. *New J. Phys.* **11**, 023002 (2009).

Acknowledgments

Author contributions

M.-H.Y., J.M. and A.A.-G. are responsible for the parts involving quantum chemistry. J.C., A.M., L.L. and E.S. are responsible for the parts involving trapped ions. All authors contributed to the writing of the paper.

Additional information